

# From progenitor to afterlife

By Roger A. Chevalier

Department of Astronomy, University of Virginia, P.O. Box 400325, Charlottesville, VA 22904, USA

The sequence of massive star supernova types IIP (plateau light curve), IIL (linear light curve), IIB, IIn (narrow line), Ib, and Ic roughly represents a sequence of increasing mass loss during the stellar evolution. The mass loss affects the velocity distribution of the ejecta composition; in particular, only the IIP's typically end up with H moving at low velocity. Radio and X-ray observations of extragalactic supernovae show varying mass loss properties that are in line with expectations for the progenitor stars. For young supernova remnants, pulsar wind nebulae and circumstellar interaction provide probes of the inner ejecta and higher velocity ejecta, respectively. Among the young remnants, there is evidence for supernovae over a range of types, including those that exploded with much of the H envelope present (Crab Nebula, 3C 58, 0540-69) and those that exploded after having lost most of their H envelope (Cas A, G292.0+1.8).

---

## 1. Introduction: Core Collapse Supernovae

Core collapse supernovae show considerable diversity among their properties. A basic observational division is into the SNe II (Type II supernovae), which have hydrogen in their spectra, and SNe Ib/c, which do not (or have weak hydrogen lines). The reason for the difference is that the progenitors of the SN Ib/c have lost their H envelopes, and perhaps more, during their evolution leading up to the supernova. The mass loss can occur either through the winds from a single star or can be aided by interaction with a binary companion.

The SNe II show strong diversity themselves. Their observational classification is based on a variety of factors, but it is clear that presupernova mass loss plays a significant role in determining the type. Two types are distinguished by their light curves: IIP (plateau) and IIL (linear). Models of Type IIP light curves have long showed that the likely progenitors of the SNe IIP are the red supergiants that end their lives with most of their H envelopes retained (Grasberg et al. 1971, Chevalier 1976). The plateau phase of the light curve is due to the internal energy deposited by the initial explosion. This progenitor hypothesis has been directly confirmed by observations of the progenitors of a number of SNe IIP (Hendry et al. 2006 and references therein). While the SNe IIP might explode with a hydrogen envelope of  $\sim 10 M_{\odot}$ , the more rapid decline of the SNe IIL imply that they explode with an envelope of  $\sim 1 M_{\odot}$  (Blinnikov & Bartunov 1993). Because of higher rates of mass loss for more luminous stars, the reduced H envelope is expected to occur for single stars with initial masses of  $\gtrsim 20 M_{\odot}$ . Alternatively, mass loss in a binary system could play a role in the reduced envelope mass.

The prototype of the SNe IIB was SN 1993J, which made a transition from a Type II at early times to a Type Ib/c at late times, based on spectroscopic observations. The H envelope mass required for SN 1993J was  $\sim 0.2 M_{\odot}$  (Woosley et al. 1994). For this to occur in a single star requires special timing, so a binary origin is preferred. A likely binary companion for SN 1993J has been directly observed (Maund et al. 2005).

SNe IIn have the spectroscopic feature of narrow emission lines (Schlegel 1990), typically  $H\alpha$ , which indicates that circumstellar interaction plays a role in the emission from early times. A supernova can be a Type IIn and another type; e.g., SN 1998S was both a IIn and IIL. Because of the strong circumstellar interaction, it can be difficult to determine the nature of the photospheric emission in a SN IIn. The H emission from

circumstellar interaction implies strong mass loss before the supernova in a SN IIn, so the H envelope is likely to be depleted at the time of the supernova.

The most noteworthy peculiar SN II is the nearby SN 1987A, which was relatively compact at the time of the explosion although it had a massive H envelope. The best explanation for the explosion as a blue supergiant star and the axisymmetric ring features around it is probably that it was in a binary system (Podsiadlowski 1992).

The Type Ib/c supernovae are believed to be H-poor Wolf-Rayet stars at the time of their explosion. There is some observational evidence that SNe Ib, which have He lines, can have a small amount of high velocity H at the time of the explosion (Elmhamdi et al. 2006). Although the presence of a H envelope in a massive star typically leads to the formation of a red supergiant in the late evolutionary stages, a small amount of H mass ( $\lesssim 0.01 M_{\odot}$ ) is not expected to support an extended envelope.

These considerations show that a major factor in the determination of supernova type is the amount of H left in the envelope at the time of the supernova. If the H envelope mass is greater than the core mass, then the core is effectively decelerated by the envelope and there is mixing between them by Rayleigh-Taylor instabilities. There is not only the outward mixing of heavy elements, but also the inward mixing of H to low velocities. This can be directly observed in the late spectra of SNe IIP; e.g., late spectra of SN 1999em showed H moving at several 100 km s<sup>-1</sup> (Elmhamdi et al. 2003).

The relative numbers of the different kinds of supernovae is uncertain from an observational point of view. If all the supernovae came from single stars, the stellar mass function was the Salpeter function ( $n(M) \propto M^{-2.35}$ ), and Type IIP supernovae came from 8 – 20  $M_{\odot}$  stars, Type IIL 20 – 25  $M_{\odot}$ , and Type Ib/c > 25  $M_{\odot}$ , the relative fractions of IIP:IIL:Ib/c would be 0.71:0.08:0.21. Binary evolution could increase the relative number of IIL and Ib/c events (Nomoto et al. 1996). However, SNe IIP are likely to be an important component of the core collapse supernovae.

After the explosion of the progenitor star, the event has an afterlife in two ways: through its interaction with the surrounding medium and through the possible activity of a central compact remnant (neutron star or black hole). I will discuss how the expectations for the afterlife phases depend on the supernova type and what can be learned about these phases from observations. The early circumstellar interaction observed in extragalactic supernovae is discussed in Section 2, the pulsar wind nebula expansion inside the supernova in Section 3, and circumstellar interaction in young remnants in Section 4. More details on the material in Sections 3 and 4 can be found in Chevalier (2005). Section 5 contains a discussion of future prospects.

## 2. Early Circumstellar Interaction

Circumstellar interaction begins soon after the supernova shock wave has emerged from the progenitor star. The radiation dominated shock front accelerates out the outer edge of the star until the point where radiative losses halt the acceleration process. Because more compact stars have a larger density contrast between the average density and the photospheric density, the shock waves attain higher velocities in more compact stars. The shock break-out radiation accelerates the gas out ahead of the shock, so that the shock front in fact disappears. However, the velocity of the radiatively accelerated gas declines with radius ( $\propto r^{-2}$ ), so that a viscous shock eventually forms. The shocked region is driven by the supernova gas, which has a steep power law profile in the region where shock acceleration has occurred. The interaction region is bounded by a reverse shock, where the supernova gas is shocked, on the inside and a forward shock, where the circumstellar gas is shocked, on the outside. If both the supernova density profile

and the surrounding wind density profile can be described as power laws in radius, the structure and evolution of the interaction region can be described by a self-similar solution (Chevalier 1982).

The early interaction in extragalactic supernovae can be observed in a number of ways: radio emission from shock accelerated electrons, X-ray emission from hot gas and nonthermal processes, optical emission from cooling shock waves and radiatively heated gas, and infrared emission from radiatively or shock heated dust grains. Radio is the best marker of interaction because it has been observed from all the types of massive star supernovae (Weiler et al. 2005). On the other hand, radio emission has never been detected from SNe Ia.

Although there is not a good understanding of particle acceleration and magnetic field generation associated with shocked regions, simple models that assume that some fraction of the postshock energy density goes into relativistic electrons and magnetic field do a reasonable job of reproducing the observed evolution of radio supernovae. Shock compression of a stellar wind magnetic field is typically not adequate (unless the magnetic field completely dominates the wind energy flux), so field amplification in the shocked region is required. Possible mechanisms for amplification are hydrodynamic instabilities in the shocked region or field amplification associated with cosmic ray driven turbulence in the shock wave (Bell 2004). An additional factor in radio light curves is early low frequency absorption of the radio emission, as is typically observed. The expected mechanisms are synchrotron self-absorption and free-free absorption by unshocked stellar wind gas.

A basic aspect of a radio light curve is thus the peak luminosity and the time of the peak. Values are shown in Fig. 1 for those supernovae that have light curves. The dashed lines in Fig. 1 result from a synchrotron self-absorption interpretation of the rise at radio wavelengths; the assumption of equipartition of energy between relativistic electrons and magnetic fields gives the radius, and thus the velocity, of the radio emitting region. Although equipartition is by no means guaranteed, the results are not sensitive to this assumption. If some process other than synchrotron self-absorption is the dominant absorption process, the radio turn-on is further delayed and the indicated velocity is lower than actually present in the supernova. This is the reason that some of the SNe II have very low apparent velocities; the turn-on is likely due to free-free absorption.

The supernovae divide themselves into 3 main regions with regard to velocity. The SNe II have the lowest velocities, although not actually as low as indicated by Fig. 1. The SNe Ib/c probably are dominated by synchrotron self-absorption and their typical velocities are  $\sim 30,000 \text{ km s}^{-1}$ . There are 3 reasons for the higher velocities in the SNe Ib/c vs. SNe II: shock acceleration during the supernova continues to higher velocities in the SNe Ib/c because of the more compact progenitors, the lower circumstellar densities around the SNe Ib/c give less deceleration of the interaction region, and the SNe Ib/c typically have lower ejecta masses than, but similar energies to, the SNe II so the ejecta have higher mean velocities.

Fig. 1 also shows the relatively nearby GRB (gamma-ray burst) – SN Ic associations. They require relativistic or semi-relativistic velocities and thus distinguish themselves from the normal SNe Ib/c. They do not have especially low ejecta mass ( $\sim 6 M_{\odot}$  was deduced for SN 1998bw, Woosley et al. 1999), so the high velocity must be due either to an extraordinarily large supernova energy or to a different source for the emission, a central GRB engine.

Among the SNe II, the range in radio luminosity is probably due to a range in mass loss density. At the low luminosity end are the SNe IIP, which have been detected only in recent years. The mass loss rates that are implied by the radio (and X-ray) observations

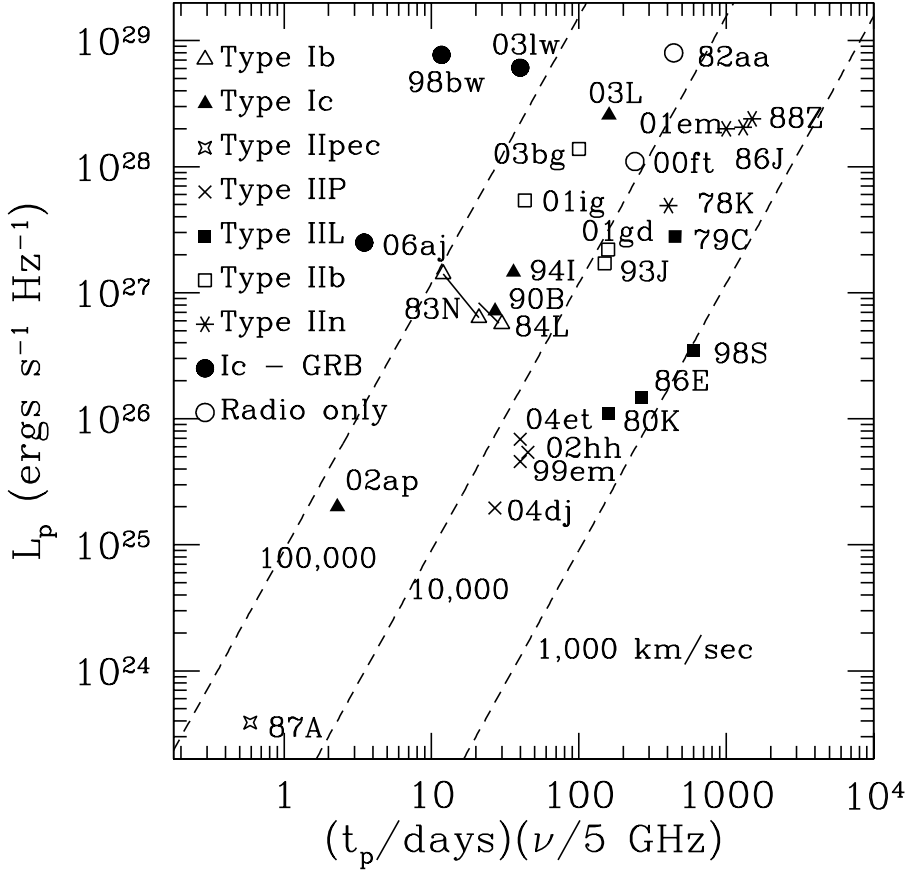


FIGURE 1. Peak radio spectral luminosity vs. the product of the time of peak and the frequency of the measurement. The observed supernovae are designated by the last two digits of the year and the letter, and the Types are indicated by the symbols. The dashed lines show the mean velocity of the radio shell if synchrotron self-absorption is responsible for the flux peak; a value of the energy index  $p = 2.5$  is assumed. This is an update of Fig. 4 of Chevalier (1998).

are consistent with those suggested by stellar evolution calculations, which are deduced from observations of Galactic stars (Chevalier, Fransson & Nymark 2006). Even over the mass range  $10 - 20 M_{\odot}$ , there is a considerable range of mass loss rate. The existing data are consistent with the expected correlation between mass loss rate and progenitor mass determined from direct observations, although there are not yet enough data to provide a good test.

The SNe IIL have a higher mass loss rate, as expected if they came from single stars. If binaries play a role, the expected mass loss rates are not so clear. At the high radio luminosity end of the SNe II are the SNe IIn, which appear to have massive, clumpy circumstellar media. In order to obtain the high radio, X-ray, and optical luminosities, the progenitor star must have lost several  $M_{\odot}$  within  $\sim 10^3$  years of the supernova.

Results on mass loss densities are summarized in Table 1, where  $\dot{M}$  is the mass loss rate and  $v_w$  is the wind velocity of the progenitor; supernova observations just give the ratio  $\dot{M}/v_w$ , so the value of  $v_w$  has been assumed. For the SNe II (except for SN 1987A), free-free absorption is the likely absorption process, so there is a fairly direct estimate of

---

SN	$\dot{M}$ ( $M_{\odot} \text{ yr}^{-1}$ )	Assumed $v_w$ ( $\text{km s}^{-1}$ )
IIP	$10^{-6} - 10^{-5}$	10
IIL	$10^{-5} - 10^{-4}$	10
93J (I Ib)	$3 \times 10^{-5}$	10
IIn	$\lesssim 10^{-3}$	10
87A (IIpec)	$4 \times 10^{-8}$	500
Ib/c	$10^{-6} - 10^{-4}$	1000

---

TABLE 1. Estimates of  $\dot{M}$  for the supernova progenitors

the circumstellar density, although uncertainties arise because of the dependence of the absorption on the circumstellar temperature.

For the SNe I Ib, Table 1 just lists the well-studied SN 1993J, which had a red supergiant progenitor. Fig. 1 shows that SN 2001gd was probably similar. However, the radio observations of SN 2001ig and SN 2003bg indicate higher velocity expansion and they probably had Wolf-Rayet star progenitors (Ryder et al. 2004, Soderberg et al. 2006). There is presumably a continuous distribution between the SNe I Ib, in which the H lines are clearly visible in spectra, and the SNe Ib, in which the H $\alpha$  line is weak.

The position of SN 1987A in Fig. 1 is determined by the low luminosity radio emission that was observed over the first 200 days after the explosion (Turtle et al. 1987). The initial rise of the radio emission is likely due to synchrotron self-absorption, so estimates of mass loss density are uncertain, but, if the efficiency of synchrotron production is similar to that for the SNe Ib/c (see below), the density is remarkably low (Table 1). This low density is supported by the rapid expansion that the supernova shock wave made to the time that the first radio imaging observations were carried out (Gaensler et al. 1997).

Since 1990, the radio flux from SN 1987A has been rising because of its interaction with mass lost during a previous red supergiant stage. This increase was anticipated by the observation of dense gas that had been radiatively illuminated and the ensuing interaction has been observed over a broad wavelength range (McCray 2005). The transition from red supergiant to blue supergiant explosion took  $\sim 10^4$  years. The radio light curve of SN 1987A is unusual because of its previous red supergiant phase, although few radio supernovae are followed past an age of 3 years. Another object that seems to have made a transition to dense gas interaction is SN 2001em, which was initially observed as a SN Ib/c and within 3 years made a transition to SN IIn, at which time it was a luminous radio and X-ray source (Chugai & Chevalier 2006 and references therein). In this case, there was apparently a phase of dense mass loss within  $\sim 10^3$  years of the supernova explosion which ended before the supernova occurred.

Like the SNe II, the SNe Ib/c also have a considerable range in peak radio luminosity (Fig. 1). The observed range in luminosity is roughly consistent with the observed range of mass loss densities for Galactic Wolf-Rayet stars if the efficiency factors (fractions of postshock energy density in magnetic fields and relativistic electrons) do not vary greatly between objects and are  $\sim 0.1$ . In this picture, SN 2002ap and SN 2003L roughly represent the low and high extremes for the radio luminosities expected for SNe Ib/c. The low density around SN 2002ap is a factor in the high velocity of the radio region that is inferred for this source.

In addition to radio emission, X-ray emission has been detected from essentially all

types of massive star supernovae, except perhaps SNe Ib. However, there is typically only a small amount of data for any particular supernova, so that the X-ray data can provide a consistency check on deductions from the radio emission, but do not yield much additional information on the mass loss properties of the progenitors. In the case of SNe II, the X-ray emission is likely to be thermal emission from the shocked ejecta gas. The interpretation of the emission generally depends on the density structure of the supernova. In the case of SNe Ib/c, the thermal interpretation generally does not produce sufficient luminosity, so nonthermal mechanisms are indicated (Chevalier & Fransson 2006). Near maximum optical light, inverse Compton emission can be important, but it cannot explain later emission. Chevalier & Fransson (2006) suggested that the late emission can be explained by synchrotron radiation in a scenario where the forward shock wave is cosmic ray dominated so that the electron energy spectrum flattens at high energy. More detailed observations are needed to check on this hypothesis.

Optical emission from circumstellar interaction occurs if the interaction is sufficiently dense to produce a radiatively cooling reverse shock wave. It is in this case that a significant fraction of the interaction power can appear at optical wavelengths. Thus, optical emission from interaction is detected from IIn, III, and IIb supernovae, but not from IIP or Ib/c supernovae. The  $H\alpha$  line profiles observed for III and IIb supernovae typically have the boxy shape that is expected for emission from a fairly narrow region near the reverse shock front. The SNe IIn have narrow centrally peaked  $H\alpha$  emission that is likely to be from slow shock waves driven into circumstellar clumps, although a detailed theory for the formation of such lines is not yet available.

Overall, there is reasonable agreement between the circumstellar media inferred from supernova observations with what is expected around the progenitor. One area of uncertainty is still what are the expectations where binary interaction has been important for the progenitor. In addition, the supernova observations are sensitive to clumping in the circumstellar wind and may provide a method to investigate clumping in winds from late type stars (e.g., Weiler et al. 2005).

### 3. Pulsar Wind Nebulae

Massive stars undergo core collapse at the end of their lives, leading to the formation of a neutron star or black hole. If the neutron star is an active pulsar, the magnetic field and relativistic particles generated by the pulsar create a bubble within the supernova (Fig. 2). Because the supernova gas is already freely expanding, the swept up shell around the bubble accelerates with time and is thus subject to Rayleigh-Taylor instabilities. This picture provides a reasonable account of the properties of the Crab Nebula (Chevalier 1977). A similar model applied to 9 young pulsar nebulae is also in accord with the observations, provided that the relativistic particles and magnetic fields are not far from equipartition in the pulsar nebulae (Chevalier 2005). In these models for the pulsar nebulae, the initial rotation periods of the pulsars are in the range 10–100 ms.

The fact that the pulsar nebula interacts with the inner part of the supernova ejecta gives constraints on the supernova type. As discussed in Section 1, the basic supernova types are related to the amount of H envelope that is lost leading up to the explosion. In SNe IIP, with most of their H envelope intact, the core material is slowed by the envelope material and the reverse shock wave during the supernova drives H rich material back towards the center of the supernova. Once the H envelope has a mass less than that of the core, it does not effectively decelerate the core material and ends up at a high velocity. While the H can give indications of the amount of mass loss, the heavy element production is related to the initial mass of the star. Below  $\sim 12 M_{\odot}$ , most of the heavy

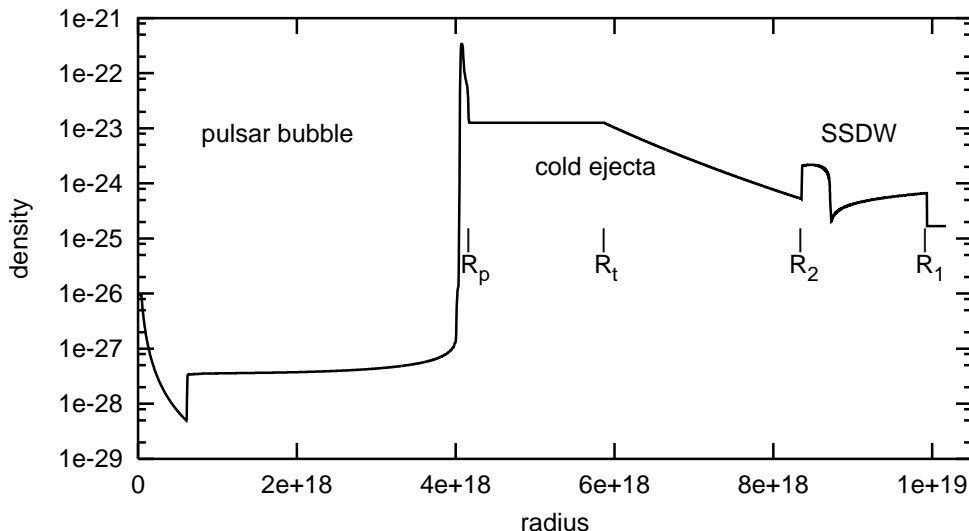


FIGURE 2. The density profile for the interaction of a pulsar nebula with the host supernova remnant. The supernova remnant is modeled as a self-similar driven wave (SSDW) bounded by a forward shock at  $R_1$  and a reverse shock at  $R_2$ . The pulsar bubble has swept up a thin shell of ejecta at  $R_p$ . The freely expanding, cold ejecta have an inflection point in the density at  $R_t$ . The reverse shock wave has not yet reached the pulsar bubble. (from Blondin, Chevalier & Frierson 2001)

elements synthesized during the stellar evolution end up in the compact object; above this mass, there are increasing amount of O (oxygen) and other heavy elements.

When the pulsar bubble expands into the supernova, there is a shock wave driven in the ejecta. During the early phases of evolution, the shock is a radiative shock, which can give optical emission. The shock emission declines either because the decreasing density and increasing shock velocity cause a transition to a nonradiative shock or because the pulsar power declines strongly so that the shell expansion tends toward free expansion. An alternative source of optical emission is photoionization of the cool gas by the ultraviolet synchrotron radiation from the pulsar bubble.

There are 3 nebulae where the swept up gas has apparently been observed: the Crab Nebula, 3C 58, and 0540–69 in the Large Magellanic Cloud. The Crab is especially well studied and shows filaments that are primarily composed of H and He, with not much in the way of heavier elements beyond those present in cosmic abundances. The small amount of heavy elements suggests a relatively low initial mass, perhaps  $8 - 10 M_{\odot}$  (Nomoto et al. 1982). The average velocity of the optical filaments is  $\sim 1400 \text{ km s}^{-1}$  and the gas was probably at a lower velocity before being accelerated by the pulsar bubble. The low velocity of the H is suggestive of a SN IIP in which the H has been mixed back toward the center; this type is also consistent with the estimated initial mass.

The optical filaments in 3C 58 are faint and more difficult to observe, but show lines of H and N, and velocities up to  $\sim 1000 \text{ km s}^{-1}$  (Fesen, Kirshner, & Becker 1988). These appear to be swept up ejecta, as opposed to shocked circumstellar gas, because of their relatively high velocities and the fact that they appear in projection only over the pulsar nebula. As in the case of the Crab, the evidence points to a relatively low mass progenitor and a SN IIP. Although 3C 58 has typically been identified with SN 1181, there are a number of lines of evidence that it is actually  $\sim 2500$  years old (Chevalier 2005).

The case of 0540–69 is different because strong lines of O and S are present. The

presence of H in the filaments has been controversial and it was assumed not to be present in Chevalier (2005), but recent observations definitely show that it is in the filaments around the pulsar bubble (Serafimovich et al. 2005), which have velocities  $\sim 1000 \text{ km s}^{-1}$ . The composition suggests an initial mass  $\gtrsim 15 M_{\odot}$  and a SN IIP, which would place the supernova among the higher mass SNe IIP.

#### 4. Young Remnants

Nearby young remnants with ages up to several 1000 years are expected to still be interacting with the mass loss region set up by the progenitor. However, the mass loss region is probably beyond the region of the free wind from the progenitor star, so the stellar evolution leading up to the supernova is important. When massive stars are on the main sequence, their fast winds can create large wind bubbles around them. The lower mass stars have lower mass loss rates, but this is partially compensated by their longer evolutionary lifetimes. The wind bubbles eventually slow to  $10 - 20 \text{ km s}^{-1}$ , which is comparable to the space velocities of the massive stars, so that they can catch up to the bubble on one side.

After the main sequence phase, stars enter the red supergiant phase, with slow ( $\sim 10 \text{ km s}^{-1}$ ), dense mass loss. The free wind extends out to the point where the wind ram pressure equals the pressure in the surrounding medium,  $p$ , i.e. at

$$r_{RSG} = 5.0 \left( \frac{\dot{M}}{5 \times 10^{-5} M_{\odot} \text{ yr}^{-1}} \right)^{1/2} \left( \frac{v_w}{15 \text{ km s}^{-1}} \right)^{1/2} \left( \frac{p/k}{10^4 \text{ cm}^{-3} \text{ K}} \right)^{-1/2} \text{ pc}, \quad (4.1)$$

where  $k$  is Boltzmann's constant. This shows that the red supergiant wind can extend out  $> 5 \text{ pc}$  from the supernova. The extended wind around SN 1987A was observed as it was illuminated by the radiation from the supernova, out to a radius  $\sim 5 \text{ pc}$  (Chevalier & Emmering 1989, Sugerman et al. 2005).

The supernova interaction with a red supergiant wind can last for 1000's of years if the wind is strong and extended, and gives rise to strong radio and X-ray emission. The best case of such interaction appears to be the 325 year old remnant Cas A. The morphology, expansion rates, and masses are consistent with interaction with a freely expanding wind (Chevalier & Oishi 2003, Laming & Hwang 2003). The remnant contains slow moving shocked circumstellar clumps, called the quasi-stationary flocculi, that are H and He rich. The fact that these give rise to narrow line emission means that Cas A can be regarded as a very old SN IIn. Whether it was a SN IIn in its early phases depends on how far back to the progenitor star the wind extended. If the progenitor made a transition to a Wolf-Rayet star before the supernova, it would have initially been a SN Ib/c. Chevalier & Oishi (2003) argued that the wind extended back to near the surface based on 2 points: there are some fast knots containing H, showing that the progenitor had some H at the time of the explosion and the formation of very fast cool knots might be aided by the presence of a dense surrounding wind. However, the knots with H in Cas A have velocities  $\sim 10,000 \text{ km s}^{-1}$  and SNe Ib can have H with velocities  $\gtrsim 12,000 \text{ km s}^{-1}$  (Elmhamdi et al. 2006).

A general expectation of strong interaction with a red supergiant wind is that enough of the H envelope has been lost that no H in the ejecta is expected at low ( $\lesssim 3000 \text{ km s}^{-1}$ ) velocity. This is the case for the fast ejecta knots in Cas A. A remnant with strong circumstellar interaction and a pulsar wind nebula is G292.0+1.8, which also has fast moving knots without H. Another remnant is 1E 0102.2-7219 in the Small Magellanic Cloud, which also has strong interaction and H-poor fast knots.

As discussed in the previous section, the suggested type of supernova for the Crab and 3C 58 is a low mass SN IIP. However, in these cases, there has been no detection of interaction with the circumstellar medium; quite strong limits have been placed on X-ray emission from interaction around the Crab nebula (Seward, Gorenstein & Smith 2006). A possible explanation for the low emissivity is that the supernova shock wave has passed through the red supergiant wind, which did not extend out far from the progenitor in this case, and is currently moving in a low density wind bubble left from the main sequence phase. Some support for this picture comes from the observation of a faint X-ray shell around the pulsar wind nebula G21.5–0.9 (Matheson & Safi-Harb 2005, Bocchino et al. 2005). This remnant was regarded as a pure pulsar nebula, like the Crab, until long X-ray observations were undertaken with *Chandra*.

Chevalier (2005) suggested that the remnant 0540–69 came from a SN Ib/c based on the apparent rapid expansion of the outer ejecta, which implied a low circumstellar density in the region surrounding the progenitor. However, as discussed in Section 3, H is present in the slow moving ejecta, which implies a IIP supernova. In this case, the interaction that is observed at a radius of 6 – 10 pc is probably with the interstellar medium; Hwang et al. (2001) estimate that mass of X-ray emitting gas is  $\sim 40 M_{\odot}$ . The fact that the X-ray temperature is relatively low for the average shock velocity suggests that the remnant is interacting with clumps or clouds. The problem with the IIP designation is the rapid expansion despite the expected interaction with the slow wind from the red supergiant progenitor. This issue requires more investigation.

## 5. Discussion and Conclusions

There are excellent future prospects for developing a more complete picture of the massive star evolution leading up to a supernova and the subsequent expansion of the supernova into the circumstellar medium. The increasing number of *Hubble Space Telescope* images of galaxies has improved the prospects for identifying the progenitor stars of nearby supernovae. Follow up observations at radio and X-ray wavelengths can then reveal the mass loss environment for that particular progenitor.

There is a growing number of young remnants that have observed pulsar wind nebulae and/or circumstellar interaction. Many of these have been well observed at X-ray wavelengths (owing to *Chandra* and *XMM*), but are less well observed at optical and infrared wavelengths. Infrared observations seem especially important because a number of the objects have high extinction. As the amount of information increases, there is the possibility of looking for correlations between the nature of the compact object in a remnant and the nature of the surrounding supernova. An initial examination of this point (Chevalier 2005) did not reveal any correlations.

Along with these endeavors, hydrodynamic modeling of the variety of supernova events, along with their interaction with mass loss, is needed. The result will be a better understanding of the final evolution of massive stars and the variety of possible outcomes.

This research was supported in part by NSF grant AST-0307366 and NASA grant NAG5-13272.

## REFERENCES

- BELL, A. R. 2004 *MNRAS* **353**, 550.  
BLINNIKOV, S. I. & BARTUNOV, O. S. 1993 *A&A* **273**, 106.  
BLONDIN, J. M., CHEVALIER, R. A. & FRIERSON, D. M. 2006 *ApJ* **563**, 806.

- BOCCHINO, F., VAN DER SWALUW, E., CHEVALIER, R. & BANDIERA, R. 2005 *A&A* **442**, 539.
- CHEVALIER, R. A. 1976 *ApJ* **207**, 872.
- CHEVALIER, R. A. 1977 In *Supernovae* (ed. D. N. Schramm) p. 53. Reidel.
- CHEVALIER, R. A. 1982 *ApJ* **258**, 790.
- CHEVALIER, R. A. 1998 *ApJ* **499**, 810.
- CHEVALIER, R. A. 2005 *ApJ* **619**, 839.
- CHEVALIER, R. A. & EMMERING, R. T. 1989 *ApJ* **342**, L75
- CHEVALIER, R. A. & FRANSSON, C. 2006 *ApJ* **651**, in press (astro-ph/0607196).
- CHEVALIER, R. A., FRANSSON, C. & NYMARK, T. 2006 *ApJ* **641**, 1029.
- CHEVALIER, R. A. & OISHI, J. 2003 *ApJ* **593**, L23.
- CHUGAI, N. N. & CHEVALIER, R. A. 2006 *ApJ* **641**, 1051.
- ELMHAMDI, A., ET AL. 2003 *MNRAS* **338**, 939.
- ELMHAMDI, A., DANZIGER, I. J., BRANCH, D., LEIBUNDGUT, B., BARON, E. & KIRSHNER, R. P. 2006 *A&A* **450**, 305.
- FESEN, R. A., KIRSHNER, R. P. & BECKER, R. H. 1988 In *Supernova Remnants and the Interstellar Medium* (ed. R. S. Roger, & T. L. Landecker) p. 55. Cambridge.
- GAENSLER, B. M., MANCHESTER, R. N., STAVELEY-SMITH, L., TZIOUMIS, A. K., REYNOLDS, J. E. & KESTEVEN, M. J. 1997 *ApJ* **479**, 845.
- GRASBERG, E. K., IMSHENIK, V. S. & NADYOZHIN, D. K. 1971 *Ap. Sp. Sci.* **10**, 28.
- HENDRY, M. A., ET AL. 2006 *MNRAS* **369**, 1303.
- LAMING, J. M. & HWANG, U. 2003 *ApJ* **597**, 347.
- HWANG, U., PETRE, R., HOLT, S. S. & SZYMKOWIAK, A. E. 2001 *ApJ* **560**, 742.
- MATHESON, H. & SAFI-HARB, S. 2005 *Adv. Sp. Res.* **35**, 1099.
- MAUND, J. R., SMARTT, S. J., KUDRITZKI, R. P., PODSIADLOWSKI, P. & GILMORE, G. F. 2005 *Nature* **427**, 129.
- MCCRAY, R. A. 2005 In *Cosmic Explosions, On the 10th Anniversary of SN1993J* (ed. J. M. Marcaide & K. W. Weiler) p. 77. Springer.
- NOMOTO, K., SUGIMOTO, D., SPARKS, W. M., FESEN, R. A., GULL, T. R. & MIYAJI, S. 1982 *Nature* **299**, 803.
- NOMOTO, K., IWAMOTO, K., SUZUKI, T., POLS, O. R., YAMAOKA, H., HASHIMOTO, M., HOFLICH, P. & VAN DEN HEUVEL, E. P. J. 1996 In *Compact Stars in Binaries* (ed. J. van Paradijs, E. P. J. van den Heuvel & E. Kuulkers) p. 119. Kluwer.
- PODSIADLOWSKI, E. M. 1992 *PASP* **104**, 717.
- RYDER, S. D., SADLER, E. M., SUBRAHMANYAN, R., WEILER, K. W., PANAGIA, N. & STOCKDALE, C. 2004 *MNRAS* **349**, 1093.
- SCHLEGEL, E. M. 1990 *MNRAS* **244**, 269.
- SERAFIMOVICH, N. I., LUNDQVIST, P., SHIBANOV, YU. A. & SOLLERMAN, J. 2005 *Adv. Sp. Res.* **35**, 1106.
- SEWARD, F. D., GORENSTEIN, P. & SMITH, R. K. 2006 *ApJ* **636**, 873.
- SODERBERG, A. M., CHEVALIER, R. A., KULKARNI, S. R. & FRAIL, D. A. 2006 *ApJ* in press (astro-ph/0512413).
- SUGERMAN, B. E. K., CROTTS, A. P. S., KUNKEL, W. E., HEATHCOTE, S. R. & LAWRENCE, S. S. 2005 *ApJS* **159**, 60.
- TURTLE, A. J., CAMPBELL-WILSON, D., BUNTON, J. D., JAUNCEY, D. L. & KESTEVEN, M. J. 1987 *Nature* **327**, 38.
- WEILER, K. W., DYK, S. D. V., SRAMEK, R. A., PANAGIA, N., STOCKDALE, C. J. & MONTES, M. J. 2005 In *1604-2004: Supernovae as Cosmological Lighthouses* (ed. M. Turatto, S. Benetti, L. Zampieri & W. Shea.) p. 290. ASP.
- WOOSLEY, S. E., EASTMAN, R. G., WEAVER, T. A. & PINTO, P. A. 1994 *ApJ* **429**, 300.
- WOOSLEY, S. E., EASTMAN, R. G. & SCHMIDT, B. P. 1999 *ApJ* **516**, 788.